Mechanism of intrinsic wavelength tuning and sideband asymmetry in a passively mode-locked soliton fiber ring laser

W. S. Man, H. Y. Tam, and M. S. Demokan

Department of Electrical Engineering, The Hong Kong Polytechnic University, Hung Hom, Kowloon, Hong Kong, China

P. K. A. Wai

Department of Electronic and Information Engineering, The Hong Kong Polytechnic University, Hung Hom, Kowloon, Hong Kong, China

D. Y. Tang

Department of Physics/Centre for Laser Science, The University of Queensland, Queensland 4072, Australia

Received March 29, 1999; revised manuscript received August 9, 1999

We have experimentally observed continuous-wavelength tuning in a passively mode-locked fiber ring laser. Depending on the polarization setting, two separated tuning ranges are observed. We show that the wavelength tuning is a result of the existence of birefringence in the laser cavity. We have also shown that the same mechanism is responsible for the power asymmetry of sidebands appearing in the soliton spectrum.
 [S0740-3224(00)01901-9]
OCIS codes: 140.4050, 140.7090, 140.3510, 060.5530.

1. INTRODUCTION

Because of their potential as compact, stable light sources of ultrashort pulses, passively mode-locked fiber ring lasers (PMFRL's) have been intensively investigated recently. Novel features such as the transform-limited soliton-pulse formation,[1,2] pulse-energy quantization,[2,3] harmonic mode locking,[4,5] and noiselike-pulse output[6,7] have been observed in the laser. In this paper we report on another intrinsic behavior of the laser; we show experimentally that by simple adjustment of the polarization controllers of the laser, the central wavelength of the mode-locked pulses can be continuously tuned. A tuning range of up to 6 nm can be achieved at ~1550 nm. Furthermore, we demonstrate that the wavelength tuning of the laser can be well understood by an analysis of the linear transmission of the laser cavity. The mechanism for the power asymmetry of the sidebands in soliton spectra of PMFRL's is also studied and explained for the first time.

The intrinsic wavelength-tuning ability of PMFRL's was mentioned in Ref. 2. However, the mechanism that is responsible for this tuning ability has not been investigated. We have investigated experimentally the wavelength-tuning mechanism of a PMFRL. We found that two discrete tuning ranges exist in the laser. Each tuning range can be obtained by a change in the polarization settings of the polarization controllers. The tuning ability and the existence of two discrete tuning ranges are found to be a result of the combined effect of the polarizer and the cavity's birefringence. The combination of a polarizer and the cavity birefringence forms a linear periodic-wavelength filter. In contrast to the cw and the actively mode-locked fiber lasers,[8,9] in order to achieve mode locking and to form a soliton in the laser cavity, the minima of the filter has to be inside the gain bandwidth of the gain medium. A mode-locked pulse is formed in the vicinity of the minima of the birefringent filter. Shifting the minima of the filter results in the wavelength tuning of the mode-locked pulses. In most of the soliton fiber lasers, the sidebands of soliton spectra were found to be asymmetric. In Ref. 10 the authors claimed that the asymmetric sidebands are due to the Raman effect, whereby the longer-wavelength sidebands are amplified by the shorter-wavelength soliton. However, Dennis and Duling[11] showed later that the strength of the shorter-wavelength sidebands can be more than the sidebands in the longer-wavelength side of the soliton spectrum. The authors explained that this sideband asymmetry is due to the nonuniformity of the amplifier's gain profile. However, we report in this paper that the asymmetric sidebands are a consequence of the filtering effect caused by the fiber birefringence.

2. EXPERIMENTAL SETUP AND RESULTS

Figure 1 shows the configuration of the soliton laser used in our experiments. The loop length of the laser cavity is ~12 m. Unidirectional operation of the laser is enforced by the inclusion of a polarization-dependent isolator (PS) in the cavity. The self-started mode locking of the laser is achieved by use of the nonlinear polarization-rotation

technique.[2,12–14] To this end two polarization controllers, one consisting of two quarter-wave plates and the other consisting of two quarter-wave plates and one half-wave plate are used to control the polarization of the light. The wave plates and the polarization-dependent isolator are mounted inside a fiber bench, which is a fiber-to-fiber coupling system used for coupling light from one fiber to another across a 7-cm open-air gap. The insertion loss (excluding the bulk-optic components) and the return isolation of the fiber bench is ~1.5 dB and ~50 dB, respectively. A 980/1550 wavelength-division-multiplexing (WDM) coupler is used to couple the pump light into the cavity. The WDM is custom designed so that 10% of the signal power (1550 nm) is also coupled out of the ring cavity, so that the signal power at the input of the erbium-doped fiber amplifier (EDFA) can be determined. A 1% output coupler is installed after the EDFA to allow the determination of the signal power after amplification. By comparison of the signal powers from these two output ports, the system transmission of the mode-locked system can be obtained. The erbium-doped fiber has an erbium concentration of 2000 parts per million (ppm). The length of the erbium-doped fiber is ~4 m long. When pumped with 90 mW of pump power, the small-signal gain of the EDFA is greater than 50 dB. The output signal of the laser is analyzed by an optical spectrum analyzer and a commercial optical autocorrelator.

By careful adjustment of the wave plates, self-started mode locking of the laser is obtained at a pump power of ~50 mW. In our experiment we characterized in detail the behavior of the laser under different operating conditions. We observed features of the laser reported by other research groups such as output-energy quantization,[2,3] sideband instability,[10,11,15,16] and harmonic mode locking.[4,5] In particular, we also found that the central wavelength of the mode-locked soliton pulses of the laser can be tuned simply by adjustment of the polarization of the polarization controllers. Figure 2 shows the experiment results observed. Two separate ranges of wavelength tuning, each spanning more than 3 nm, exist in the laser. Figure 2(a) shows a case in which the central wavelength of the soliton pulses is continuously tuned from 1552 nm to 1558 nm, and Fig. 2(b) shows the central wavelength as continuously tuned from 1562 nm to 1565 nm. The two separate wavelength-tuning ranges are obtained with different polarization settings of the polarizers. In both cases the wavelength tuning is achieved simply by rotation of one of the wave plates in the polarization controller; there is no adjustment to the pump power.

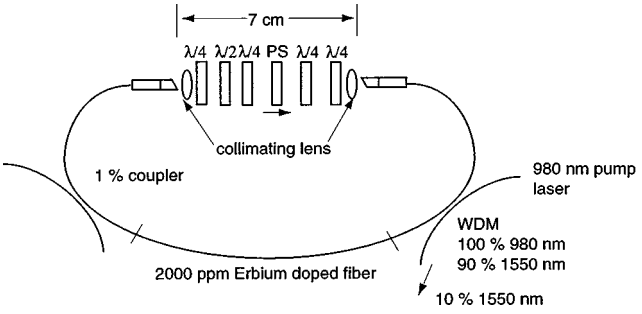

Fig. 1. Experimental setup of the compact soliton laser: λ/4, quarter-wave plate; λ/4, half-wave plate; PS, polarization-dependent isolator.

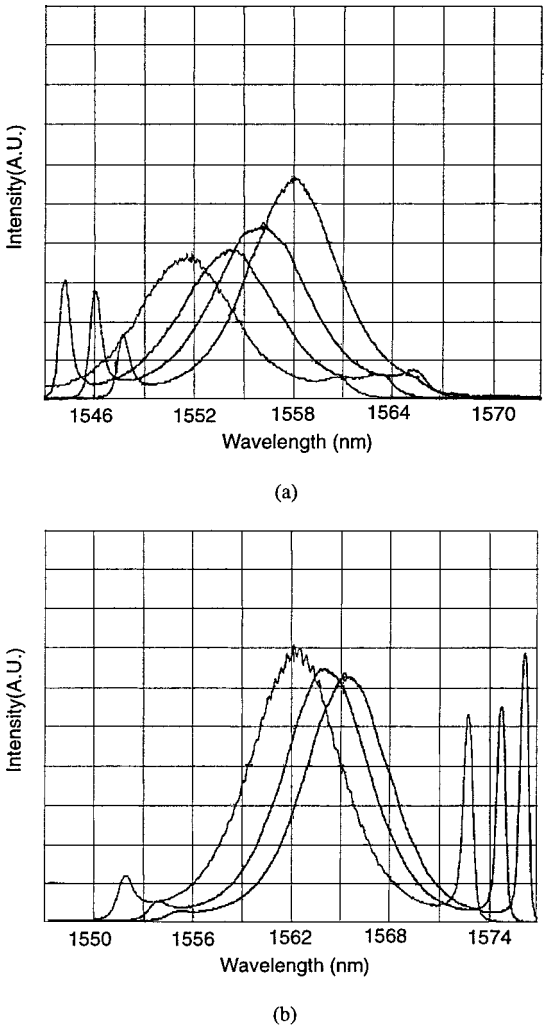

Fig. 2. Spectrum of the mode-locked output obtained from the soliton laser: (a) and (b) show the two separate ranges of wavelength tuning.

It should be noted that the strength of the sidebands shown in Fig. 2 is asymmetric. In all of our experiments we observed this asymmetry. Although the powers of the shorter-wavelength sidebands in Fig. 2(a) are stronger, the sidebands in Fig. 2(b) are stronger on the longer-wavelength side.

3. LINEAR CAVITY-TRANSMISSION ANALYSIS

To explain the wavelength tunability of the laser and the observed asymmetry in the sideband strength, we start by analyzing the linear transmission of the laser cavity. The transmission of the laser cavity is equivalent to a system shown in Fig. 3.[17] Assume that the polarization of the light output from the polarization-dependent isolator aligns with the *y* axis represented by the vector

$$\begin{bmatrix} 1 \\ 0 \end{bmatrix}. \tag{1}$$

The polarization controller P_1 transforms the light to an elliptical polarization state. The transformation is described by the transfer matrix

$$R_1 = \begin{bmatrix} \cos\theta_1 \exp(i\Delta\phi/2) & \sin\theta_1 \exp(i\Delta\phi/2) \\ -\sin\theta_1 \exp(-i\Delta\phi/2) & \cos\theta_1 \exp(-i\Delta\phi/2) \end{bmatrix}, \quad (2)$$

where θ_1 is the angle between the y axis and the vertical birefringent axis v and $\Delta\phi$ is the phase shift between the wave components in the two orthogonal birefringent axes v and h (see Fig. 3). Let the light propagation along the fiber be described by a matrix P. In the linear regime and when there is no gain, the propagation will introduce only a linear phase shift between the two polarization components. In this case P can be written as

$$P = \begin{bmatrix} \exp(i\Delta\phi'/2) & 0 \\ 0 & \exp(-i\Delta\phi'/2) \end{bmatrix}. \quad (3)$$

Here, $\Delta\phi' = 2\pi(1 - \delta\lambda/\lambda_s)L/L_b$ is the linear phase shift between two polarization components. λ_s is the signal wavelength, and $\delta\lambda$ is the wavelength detuning. L_b is the birefringence beat length. At the end of the fiber the analyzer PA projects the light onto its axes. The action is described by the matrix R_2:

$$R_2 = \begin{bmatrix} \cos\theta_2 & \sin\theta_2 \\ -\sin\theta_2 & \cos\theta_2 \end{bmatrix}. \quad (4)$$

Here θ_2 is the angle between the axes of the analyzer and the vertical birefringent axis v. The total transformation is then given by

$$T = \begin{bmatrix} \cos\theta_1\cos\theta_2 \exp[i(\Delta\phi/2 + \Delta\phi'/2)] - \sin\theta_1\sin\theta_2 \exp[-i(\Delta\phi/2 + \Delta\phi'/2)] \\ -\sin\theta_1\cos\theta_2 \exp[-i(\Delta\phi/2 + \Delta\phi'/2)] - \sin\theta_2\cos\theta_1 \exp[-i(\Delta\phi/2 + \Delta\phi'/2)] \end{bmatrix}. \quad (5)$$

With T_1 denoting as the transmission of the system the power transmission of the cavity is given by

$$|T_1|^2 = \cos^2\theta_1\cos^2\theta_2 + \sin^2\theta_1\sin^2\theta_2 + \frac{1}{2}\sin 2\theta_1 \sin 2\theta_2 \cos(\Delta\phi + \Delta\phi'). \quad (6)$$

Here θ_1 is assumed to be positive. From Eq. (6) one can see that the linear system transmission depends on the phase shift between the two polarization components introduced by the polarization controllers and the fiber birefringence. The peak transmission depends on $\Delta\theta = \theta_2 - \theta_1$. When $\Delta\theta$ is equal to 90°, the peak transmission can reach 100%. Figure 4 shows curves of the system transmission versus the total linear phase shift between the two polarization components, for $\Delta\theta$ varying from $\pi/2$ to $\pi/2 + \pi/5$, and when θ_1 is equal to 45°.

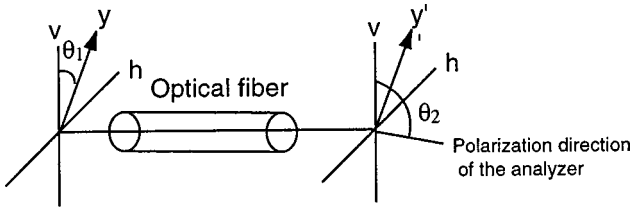

Fig. 3. Illustration of the polarization state of the light in the mode-locked system.

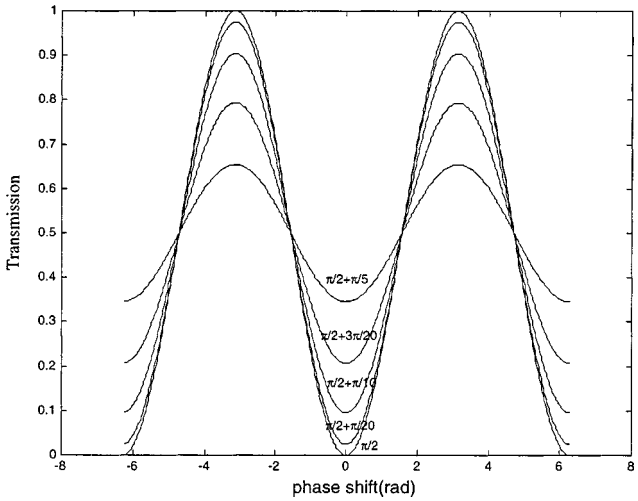

Fig. 4. System transmission of the soliton ring laser versus the phase shift between two orthogonal-polarization components when $\theta_2 - \theta_1$ varies from $\pi/2$ to $(\pi/2 + \pi/5)$ and $\theta_1 = 45°$.

The figure shows that the maximum linear system loss occurs at positions where the total linear phase shift between the two polarization components is an integer multiple of 2π rad. When the phase shift is off from this angle, the system transmission increases. Therefore, if one sets the polarization controllers such that the light at a particular wavelength λ is within the gain bandwidth of the EDFA and satisfies this condition, mode locking can occur because the nonlinear refractive index changes the phase shift between the two polarization components. Figure 4 also shows that when $\Delta\theta$ is offset from 90°, the difference between the peak transmission and the minimum transmission of the system is decreased. This means that the mode-locked pulse will be less stable because the cw is not effectively rejected. In fact, we have observed some unstable mode-locking spectra in our experiment. These unstable mode-locking regimes are usually very easy to obtain, since the contrast between the linear and the nonlinear system transmission is small when compared with the stable mode-locking regime. Therefore an easy way to obtain a stable mode-locked pulse is first to obtain the unstable mode-locked spectrum by adjustment of the polarization controllers in a coarse manner and then by tuning of the laser to the stable mode-locking regime by fine adjustment of them.

We now consider the wavelength-dependent transmission characteristic of this system. Figure 5 shows the linear system transmission against the wavelength shifted from the minimum transmission wavelength, for the cases of cavity length equal to 1, 5, and 10 beat lengths. The figure clearly shows that the bandwidth of the system transmission decreases with the birefrin-

gence. This is an analogy for how the group delay owing to birefringence prevents the short-pulse formation in the laser.[6,7] Therefore to obtain a shorter pulse, which means larger bandwidth, a smaller birefringence in the laser cavity is required. Owing to the dispersive nature of the system, the central wavelength of the mode-locked pulse is not determined solely by the spectral gain profile of the EFDA. One can see from Eq. (6) that the system transmission is a periodic function of the wavelength shift $\delta\lambda$ and the phase difference between the two orthogonal polarization components $\Delta\phi$ introduced by the polarization controllers. Therefore the linear-transmission minimum can be shifted around within the gain–bandwidth by variation of $\Delta\phi$. Since the stable mode-locked wavelength is determined by the nonlinear transmission spectrum of the mode-locked system and the saturated spectral gain profile of the EDFA, the central wavelength of the mode-locked pulse can be varied by adjustment of the polarization controllers. This is confirmed by the numerical simulations in the later part of the paper.

We also found that the power asymmetry in the sidebands can be explained based on a linear cavity-transmission analysis. In the case of a laser cavity with a multibirefringent beat length, the nonlinearity of the fiber introduces a nonlinear phase change[12,13,17]:

$$\Delta\phi_{\text{nonlinear}} = \frac{2\gamma L}{3} P \cos(2\theta_1), \tag{7}$$

in the form of a cosine function in Eq. (6), where P is the instantaneous peak power of the signal and γ is the fiber nonlinearity. Depending on the initial projection angle (θ_1) of the light with respect to the fast axis, the nonlinear phase shift ($\Delta\phi_{\text{nonlinear}}$) can be either negative or positive (positive when $0 < \theta_1 < 45°$ and negative when $45 < \theta_1 < 90°$). If $\Delta\phi_{\text{nonlinear}}$ is positive (negative), the transmission in the shorter (longer) -wavelength side of λ_s will increase, whereas the transmission in the longer (shorter) wavelength side will decrease, as can be seen from Eq. (6). So the light in shorter (longer) -wavelength side of λ_s will experience an effective saturable absorber for positive (negative) $\Delta\phi_{\text{nonlinear}}$. Therefore the soliton

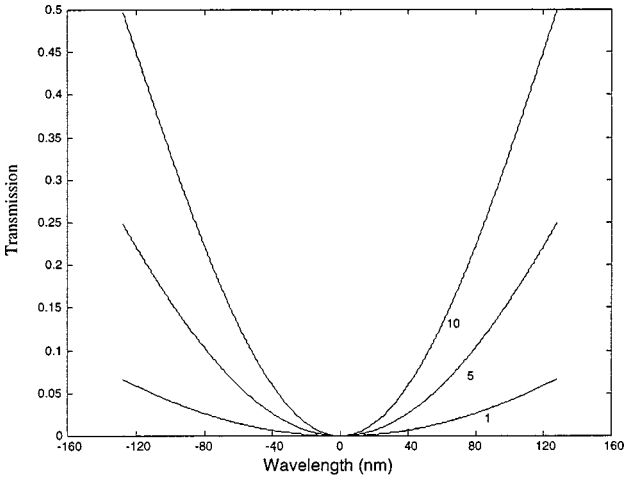

Fig. 5. System transmission versus frequency shift for a central wavelength 1550 nm, and when the system length is equal to 1, 5, and 10 beat lengths.

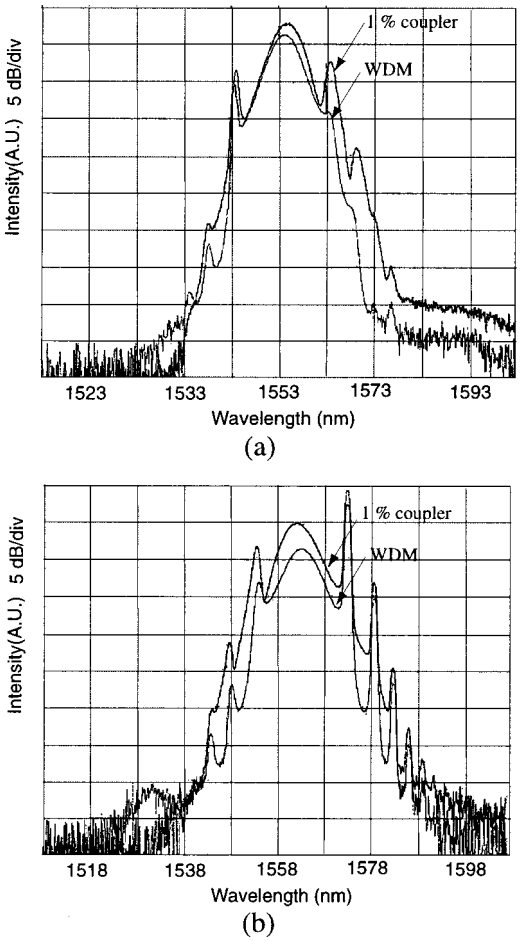

Fig. 6. Mode-locked pulse spectra measured from the WDM and a 1% output coupler when the mode-locked wavelength is (a) 1554 nm and (b) 1564 nm.

is formed in the shorter (longer) -wavelength side of λ_s if $\Delta\phi_{\text{nonlinear}}$ is positive (negative). As a consequence, the loss experienced by the sidebands in one side of the pulse spectrum will be higher than the loss in the other side because the sidebands' locations in the linear-transmission curve are asymmetric in relation to λ_s. The existence of either a positive or a negative nonlinear phase shift explains the experimentally observed sideband asymmetry.

Sidebands in the spectrum of a mode-locked pulse correspond to the small intensity pedestals of the pulse in the time domain. They are linear waves. Experimentally, one can estimate the linear system transmission by comparing the changes of sideband strength measured before and after the polarization-dependent isolator. Figure 6 shows examples of soliton spectra measured from the WDM's monitoring port and that from the 1% output coupler when the central wavelength of the mode-locked pulse is 1554 nm and 1564 nm. The mode-locked spectra in Figs. 6(a) and 6(b) were obtained from the same settings of the polarization controllers as in Figs. 2(a) and 2(b), respectively.

From Fig. 6(a) we note that the loss of the sidebands in the shorter-wavelength side of the mode-locked pulse is lower than that of the sidebands in the longer-wavelength side, whereas the transmission of the sidebands in Fig. 6(b) has the opposite characteristic. The asymmetric

sideband strength suggests strongly that the central wavelength of the mode-locked pulse is not at the minimum of the linear-transmission curve in Fig. 5. We examined the mode-locked pulse in some other wavelengths with the same settings of the two polarization controllers, and they all show similar characteristics. This experimental result also confirms that the linear loss of the system is dispersive, i.e., the linear system loss is frequency dependent.

4. NUMERICAL SIMULATIONS

To prove our analysis of the mechanism of the soliton wavelength tuning and the sideband power asymmetry, and, in particular, for an insight into the effect of nonlinear phase change, we also performed numerical simulations to study the mode locking and the soliton pulse propagation in the laser cavity. Our simulations are based on the modified coupled nonlinear Schrödinger equations[18]

$$-i\frac{\partial u}{\partial z} = \beta u + i\delta\frac{\partial u}{\partial t} + \beta''\frac{1}{2}\frac{\partial^2 u}{\partial t^2} + \gamma\left(|u|^2 u + \frac{2}{3}|v|^2 u + \frac{1}{3}v^2 u^*\right) + \frac{g_p}{2}u, \tag{8a}$$

$$-i\frac{\partial v}{\partial z} = -\beta v - i\delta\frac{\partial v}{\partial t} + \beta''\frac{1}{2}\frac{\partial^2 v}{\partial t^2} + \gamma\left(|v|^2 v + \frac{2}{3}|u|^2 v + \frac{1}{3}u^2 v^*\right) + \frac{g_p}{2}v. \tag{8b}$$

where u and v are the two linearly orthogonal polarized modes of the optical fiber. $2\beta = 2\pi\Delta n/\lambda$ is the wave-number difference (π/β is the fiber's beat length) and $2\delta = 2\beta\lambda/2\pi c$ is the inverse group-velocity difference. β'' is the dispersion parameter, and γ is the nonlinearity of the fiber.

Furthermore,

$$g_p = g_0 \Big/ \left[1 + \int (|u|^2 + |v|^2)\mathrm{d}t/E_s\right], \tag{9}$$

is the gain of the EDFA. g_0 is the small-signal peak gain and E_s is the saturation energy. For an undoped fiber, g_0 is zero. g_0 is assumed to have a spectral profile of

$$g_0(\omega) = g_0/[1 + (\omega/\Delta\omega)^n]. \tag{10}$$

Here g_0 is the peak gain, ω is the frequency detuning, and $\Delta\omega$ is the EDFA bandwidth. n is the parameter that determines the flatness of the gain profile. We used parameter values as shown in Table 1 in our simulations.

In order to closely simulate the experimental situation, especially to take into account the effects of discrete action of each cavity component, we solved the coupled nonlinear Schrödinger equations in the following way. We start our numerical simulations with a linearly polarized amplified-spontaneous-emission noise amplitude q. The noise q first travels through a polarization controller that separates it into two polarization components:

$$q_v = q\cos(\theta_1),$$

$$q_h = q\sin(\theta_1)\exp(-i\Delta\phi). \tag{11}$$

The two polarization components then propagate in the single-mode fiber according to Eqs. (8a) and (8b). To compare the simulation results with the experimental results, our simulation uses a laser-cavity configuration similar to our experimental setup. The light is first launched into a 5-m length of standard fiber (the signal arm of the WDM), followed by a 4-m erbium-doped fiber and 3 m of another standard fiber (output coupler). We did not measure the exact birefringence in the laser cavity, and the birefringence strength (beat length of ~2 m) in the cavity is a crude estimate from the sideband's transmission in Figs. 6(a) and 6(b). Although most of the laser cavity is constructed with standard single-mode fiber that has an intrinsic birefringence of $\sim 10^{-7}$ (beat length of ~10 m), there is strong birefringence from the wave plates. It has been pointed out by Horowitz *et al.* that the birefringence in the laser cavity can be very significant owing to the winding of fibers and the nonuniformities of the EDFA in the laser cavity.[6,7] This birefringence value gives a good qualitative agreement between the experimental and the simulation results. Finally, the projection of light onto the analyzer is described by

Table 1. Parameters Used in the Computer Simulation of a Soliton Laser

γ	$3\ \mathrm{W}^{-1}\,\mathrm{km}^{-1}$
β''	$15\ \mathrm{ps}^2/\mathrm{km}$
g_0	$1600\ \mathrm{km}^{-1}$
$\Delta\omega$	$4\ \mathrm{THz} \times 2\pi$
n	6
L/L_b	5
θ_2	$\theta_1 + \pi/2 - 0.05$

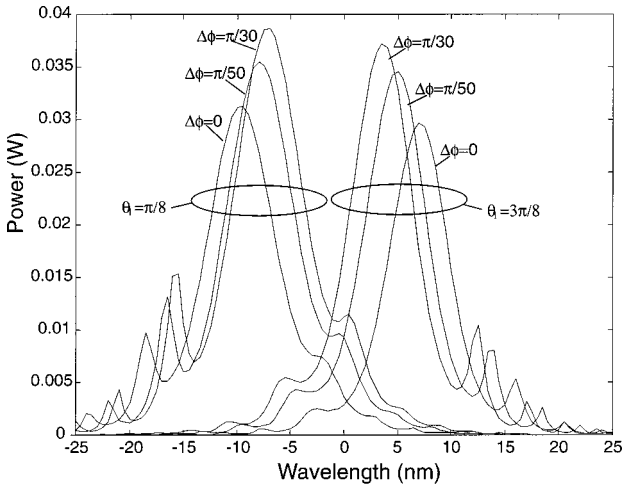

Fig. 7. Calculated spectra of the soliton pulses for the linear phase shifts $\Delta\phi$ equals 0, $\pi/50$, and $\pi/30$, when the projection angle θ_1 is chosen to be $\pi/8$ or $3\pi/8$.

$$q = q_v' \cos(\theta_2) + q_h' \sin(\theta_2), \tag{12}$$

where q_v' and q_h' are the two orthogonal polarizations components of the light after propagation in the laser cavity.

The iteration is repeated by use of the result obtained from the previous round of calculation as the initial condition. This procedure is continued until a stable mode-locking state is obtained. In our simulation the saturation energy in Eq. (9) is varied to obtain a stable single-soliton operation regime.

Figure 7 shows the pulse spectra calculated with different initial phase shifts between the fast and the slow birefringent axes. In the calculations the projection angle (θ_1) is chosen as $\pi/8$ or $3\pi/8$ ($\pi/2-\pi/8$). The figure shows that the central wavelength of the soliton spectra varies with the phase shift ($\Delta\phi$) in both cases. The obtained soliton spectra also show the power asymmetry of the sidebands, which is similar to that observed in the experiment.

5. CONCLUSIONS

In conclusion, we have found experimentally that the central wavelength of soliton pulses of a passively mode-locked soliton fiber ring laser can be continuously tuned by simple adjustment of the polarization of the polarization controllers. Two wavelength-tuning ranges exist, each with a tuning range that extends over 3 nm. On the basis of on the linear cavity-transmission analysis, we have shown that the existence of the two wavelength-tuning ranges and the continuous-wavelength-tuning ability of the soliton laser is related to the wavelength-filtering effect that results from the fiber birefringence. We have also found that the sideband asymmetry observed in the soliton-pulse spectrum is a direct consequence of the same effect.

ACKNOWLEDGMENT

This work is supported by a research grant awarded by The Hong Kong Polytechnic University.

REFERENCES

1. K. Tamura, H. A. Haus, and E. P. Ippen, "Self-starting additive pulse mode-locked erbium fibre ring laser," Electron. Lett. **28**, 2226–2228 (1992).
2. V. J. Matsas, T. P. Newton, and M. N. Zervas, "Self-starting passive mode-locked fibre ring laser exploiting nonlinear polarization switching," Opt. Commun. 61–66 (1992).
3. A. B. Grudinin, D. J. Richardson, and D. N. Payne, "Energy quantisation in figure eight fibre laser," Electron. Lett. **28**, 67–68 (1992).
4. A. B. Grudinin, D. J. Richardson, and D. N. Payne, "Passive harmonic modelocking of a fibre soliton ring laser," Electron. Lett. **29**, 1860–1861 (1993).
5. D. J. Richardson, R. I. Laming, D. N. Payne, V. J. Matsas, and M. W. Philips, "Pulse repetition rates in passive self-starting femtosecond soliton fibre laser," Electron. Lett. **27**, 1451–1453 (1991).
6. M. Horowitz, Y. Barad, and Y. Silberberg, "Noiselike pulses with broadband spectrum generated from an erbium-doped fiber laser," Opt. Lett. **22**, 799–801 (1997).
7. M. Horowitz and Y. Silberberg, "Nonlinear filtering by use of intensity-dependent polarization rotation in birefringent fibers," Opt. Lett. **22**, 1760–1762 (1997).
8. U. Ghera, N. Friedman, and M. Tur, "A fiber laser with a Comb-like spectrum," IEEE Photon. Technol. Lett. **5**, 1159–1161 (1993).
9. N. Friedman, A. Eyal, and M. Tur, "The use of the principal states of polarization to describe tunability in a fiber laser," IEEE J. Quantum Electron. **33**, 642–648 (1997).
10. N. Pandit, D. U. Noske, S. M. Kelly, and J. R. Taylor, "Characteristic instability of fibre loop soliton lasers," Electron. Lett. **28**, 455–456 (1992).
11. M. L. Dennis and I. N. Duling, III, "Experimental study of sideband generation in femtosecond fiber lasers," IEEE J. Quantum Electron. **30**, 1469–1477 (1994).
12. M. Hofer, M. E. Fermann, F. Haberl, M. H. Ober, and A. J. Schmit, "Mode locking with cross-phase and self-phase modulation," Opt. Lett. **16**, 502–504 (1991).
13. R. H. Stolen, J. Botineau, and A. Ashkin, "Intensity discrimination of optical pulses with birefringent fibers," Opt. Lett. **7**, 512–514 (1982).
14. H. G. Winful, "Self-induced polarization changes in birefringent optical fibers," Appl. Phys. Lett. **47**, 213–215 (1985).
15. D. U. Noske, N. Pandit, and J. R. Taylor, "Source of spectral and temporal instability in soliton fiber lasers," Opt. Lett. **17**, 1515–1517 (1992).
16. M. L. Dennis and I. N. Duling, "Role of dispersion in limiting pulse width in fiber lasers," Appl. Phys. Lett. **62**, 2911–2913 (1993).
17. C. J. Chen, P. K. A. Wai, and C. R. Menyuk, "Soliton fiber ring laser," Opt. Lett. **17**, 417–419 (1992).
18. S. G. Evangelides, Jr., L. F. Mollenauer, J. P. Gordon, and N. S. Bergano, "Polarization multiplexing with solitons," J. Lightwave Technol. **10**, 28–35 (1992).